J. Coat. Technol. Res., **9** (5) 503–514, 2012
DOI 10.1007/s11998-012-9397-7

Preparation, characterization and properties of UV-curable waterborne polyurethane acrylate/SiO_2 coating

Fengxian Qiu, Heping Xu, Yingying Wang, Jicheng Xu, Dongya Yang

Abstract The UV-curable waterborne polyurethane acrylate (UV-WPUA) oligomer was first prepared based on isophorone diisocyanate (IPDI), polyether polyol (NJ-220), dimethylol propionic acid (DMPA), and hydroxyethyl methyl acrylate (HEMA) via an in situ method. With the different content tetraethoxysilane (TEOS) and 3-glycidyloxypropyltrimethoxysilane (GLYMO) as coupling agents, a series of waterborne UV-WPUA/SiO_2 oligomers were prepared by the sol–gel process. The physical and mechanical properties of the UV-WPUA and UV-WPUA/SiO_2 hybrid coating materials were measured. The UV-WPUA and WPUA/SiO_2 hybrid materials were characterized using FTIR spectra, differential scanning calorimetry (DSC), thermogravimetric analysis (TGA), scanning electron microscope (SEM), transmission electron microscope (TEM), and X-ray diffraction (XRD) measuring apparatuses to determine their structures, thermal properties, surface morphologies, etc. The results showed the SiO_2 particles of the hybrid materials had wide dispersion, forming a good interfacial bonding layer on surfaces. The tensile strength, water resistance, and thermal properties of the hybrid materials were better than those of the UV-WPUA. The resulting UV-WPUA/SiO_2 hybrids are promising for a number of applications, e.g., for high-performance water-based UV-curable coatings.

Keywords Polyurethane, Hybrid, Mechanical property, Thermal property, UV-curable, Sol–gel method

F. Qiu (✉), H. Xu, Y. Wang, J. Xu, D. Yang
School of Chemistry and Chemical Engineering, Jiangsu University, Zhenjiang 212013, China
e-mail: fxqiuchem@163.com

Introduction

UV-curable coating applications have gained wide interest because of their advantages, such as few volatile organic compounds (VOC), lower energy consumption, reduced cycle time, increased production capacity, high chemical stability, and very rapid curing features at ambient temperatures. They are expected to replace solvent-based products to become the most favored domestic and industrial coatings.[1–3] In addition to these important features, this technology can offer a broad range of changes in formulation and curing conditions, and thus the final properties.

UV-curable polyurethane acrylate (PUA) aqueous coatings have been most extensively studied, have gained more and more attention and experienced speedy development in recent years because of their versatility, environmental friendliness, excellent mechanical performance, abrasion resistance, and toughness, combined with excellent resistance to chemicals and solvents. Typically, PUA is a segmented PU oligomer tipped with acrylic functionality, such as hydroxy-ethylacrylate (HEA) or hydroxyethyl methyl acrylate (HEMA). The hard segments are formed by isocyanate and HEA or HEMA, and the soft segments generally consist of polyester or polyether polyol. The immiscibility between the soft and hard segments leads to separation of the two phases, which can be prevented partly by hydrogen bonds between urethane NH and polyether (–O–) or polyester carbonyls. The degree of microphase separation has a great effect on the properties of the cured films, such as hardness, flexibility, abradability, etc. One way to improve the properties of these coatings is by the addition of inorganic particles into the organic polymeric matrix which leads, under proper conditions, to the formation of a hybrid material.

In recent years, organic–inorganic hybrid materials have attracted considerable attention due to their

enhanced coating properties, such as resistance to scratching and abrasion, thermal stability, etc. These materials also demonstrate some advantages such as low optical propagation loss, high chemical and mechanical stabilities, and good compatibility with the different surfaces to be coated.[4,5] The sol–gel route is the most commonly employed method for the preparation of organic–inorganic hybrids at the macro/microscale, even at the molecular level in mild conditions. Among the various inorganic nanosized fillers, silica nanoparticles have many advantages, including high hardness, a relatively low refractive index, and commercial availability from different sources: sols of nanosilica as colloid dispersions in water or organic solvents. In addition, silica has a silanol group on the surface, which may interact with the hard or soft segments of polyurethane, thereby aiding dispersion of the silica nanoparticles in the polyurethane matrix.[6]

The hybrid materials combine some advantages of organic polymers (easy processing with conventional techniques, elasticity, and organic functionalities) with properties of inorganic oxides (hardness, thermal and chemical stability, transparency). Karataş et al.[7] prepared a series of UV-curable organic–inorganic hybrid coating materials containing TEOS, titanium tetraisopropoxide, acetylacetone, and cycloaliphatic epoxy acrylate by the sol–gel method. The hybrid coating properties such as gloss, adhesion, tensile strength and modulus were affected by the level of silica and titania content. Huang and Hsieh[8] reported that a sol–gel chemical route was adopted to prepare zinc oxide (ZnO) nanoparticles as small as 4 nm. UV-curable ZnO-acrylic nanocomposites were then prepared by employing 3-(trimethoxysilyl)propyl methacrylate (TPMA) as the surface modification agent of ZnO particles. UV–Vis analysis revealed a high optical transparency (>95 wt%) in the visible light region for nanocomposite thin films with ZnO contents up to 20 wt%. The addition of ZnO nanoparticles also enhanced the dielectric constants of nanocomposites, and dielectric constants greater than 4 in frequencies ranging from 1 to 600 MHz were obtained in the samples containing 10 wt% of ZnO nanoparticles. Bayramoğlu et al.[9] synthesized novel hybrid oligomers based on a UV-curable epoxy acrylate resin (EA). The EA resin was modified with various amounts of the 3-isocyanatopropyl trimethoxysilane (IPTMS) coupling agent. The hybrid networks are characterized by the analysis of various properties such as hardness, gloss, the tape adhesion test, and the stress–strain test. The thermal behavior was also evaluated.

UV-curable hybrid coatings represent a major class of hybrid materials. This kind of formulation consists of one or more photosensitive organic groups, usually unsaturated C=C bonds, which can be polymerized under UV radiation. The organic oligomer can be functionalized with pending functional groups forming a second network. Hydrolysis and condensation reactions of the inorganic part and photopolymerization of the organic moieties lead to a glass-like material at room temperature. In this paper, the sol–gel derived UV-curable-WPUA/SiO_2 oligomer was prepared based on isophorone diisocyanate (IPDI), polyether polyol (NJ-220), dimethylol propionic acid (DMPA), hydroxyethyl methyl acrylate (HEMA), tetraethoxysilane (TEOS), and 3-glycidyloxypropyltrimethoxysilane (GLYMO). The effects of the TEOS content on dispersions as well as the morphology, thermal, physical, and mechanical properties of the UV-WPUA/SiO_2 hybrid coating films were investigated.

Experimental procedure

Materials

Polyether polyol (NJ-220, Mn = 2000 g/mol) was produced by Ningwu Chemical Co. Ltd. in Jurong, Jiangsu, China. Dimethylol propionic acid (DMPA) was produced by PERSTOP Co. in Helsingborg, Sweden. Isophorone diisocyanate (IPDI) was supplied by Rongrong Chemical Ltd. in Shanghai, China. 2-Hydroxyethyl methacrylate (HEMA) was provided by Yinlian Chemical Ltd. in Wuxi, Jiangsu, China. Butyl acrylate (BA), triethylamine (TEA), acetone, ethanol, dibutylbis(lauroyloxy)tin (DBTL), hydrochloric acid, tetraethoxysilane (TEOS), and *N*-methyl-2-pyrrolidone (NMP) were obtained from Sinopharm Chemical Reagent Co. Ltd. in Shanghai, China. 3-Glycidyloxypropyltrimethoxysilane (GLYMO) was purchased from Nanjing Shuguang Chemical Plant in Nanjing, China. Tripropyleneglycol diacrylate (TPGDA) and Darocur 1173 were supplied from Mingda Macromolecule Science and Technology Co. Ltd. in Suzhou, Jiangsu, China.

Preparation of UV-WPUA oligomer

Certain amounts of polyether polyol (NJ-220, 15.014 g) and isophorone diisocyanate (IPDI, 8.325 g) were added into a four-necked flask equipped with a mechanical stirrer, thermometer, and reflux condenser. Then dibutylbis(lauroyloxy)tin (DBTL) was added as a catalyst and the mixture was heated to 60°C for 2 h to prepare the –NCO terminated prepolymer. Next, the above prepolymer was reacted with a certain amount of dimethylol propionic acid (DMPA, 1.221 g) dissolved in a small amount of *N*-methyl-2-pyrrolidone (NMP) at 80–85°C for another 2 h, and the –NCO terminated prepolymer containing carboxyl group was obtained. Then the reactant was cooled down to 60°C. 2-Hydroxyethyl methacrylate (HEMA, 4.875 g) was added into the system and reacted at 60°C for 5 h. When the temperature was cooled down to 40°C, triethylamine (TEA) was added into the flask subsequently and reacted at 40°C for 30 min. The mixture was then dispersed into deionized water under vigorous

stirring for 30 min. The synthetic route of the UV-WPUA oligomer is shown in Fig. 1.

Preparation of UV-WPUA/SiO_2 hybrid oligomer

UV-WPUA/SiO_2 hybrid material oligomer containing different inorganic content was prepared via a sol–gel process.[10] In this study, a homogeneous organic solution was obtained from the coupling agent 3-glycidyloxypropyltrimethoxysilane (GLYMO) and UV-WPUA oligomer at 40°C for 1 h. The homogeneous inorganic solution was a hydrolyzed tetraethoxysilane (TEOS), which was prepared with deionized water, hydrochloric acid, ethanol, and TEOS in a conical flask, and was stirred for 1 h. Then it was added carefully to the organic solution and reacted for another 1 h. The solution was cooled to room temperature and stirred for 12 h. The precursor, GLYMO, had two different reactive functionalities, namely, the organic functional group and the inorganic alkoxysilane group. GLYMO is one of the most popular coupling agents; it can serve as a bridging unit by forming interphase links through the hydrolysis and condensation of the trialkoxysilane

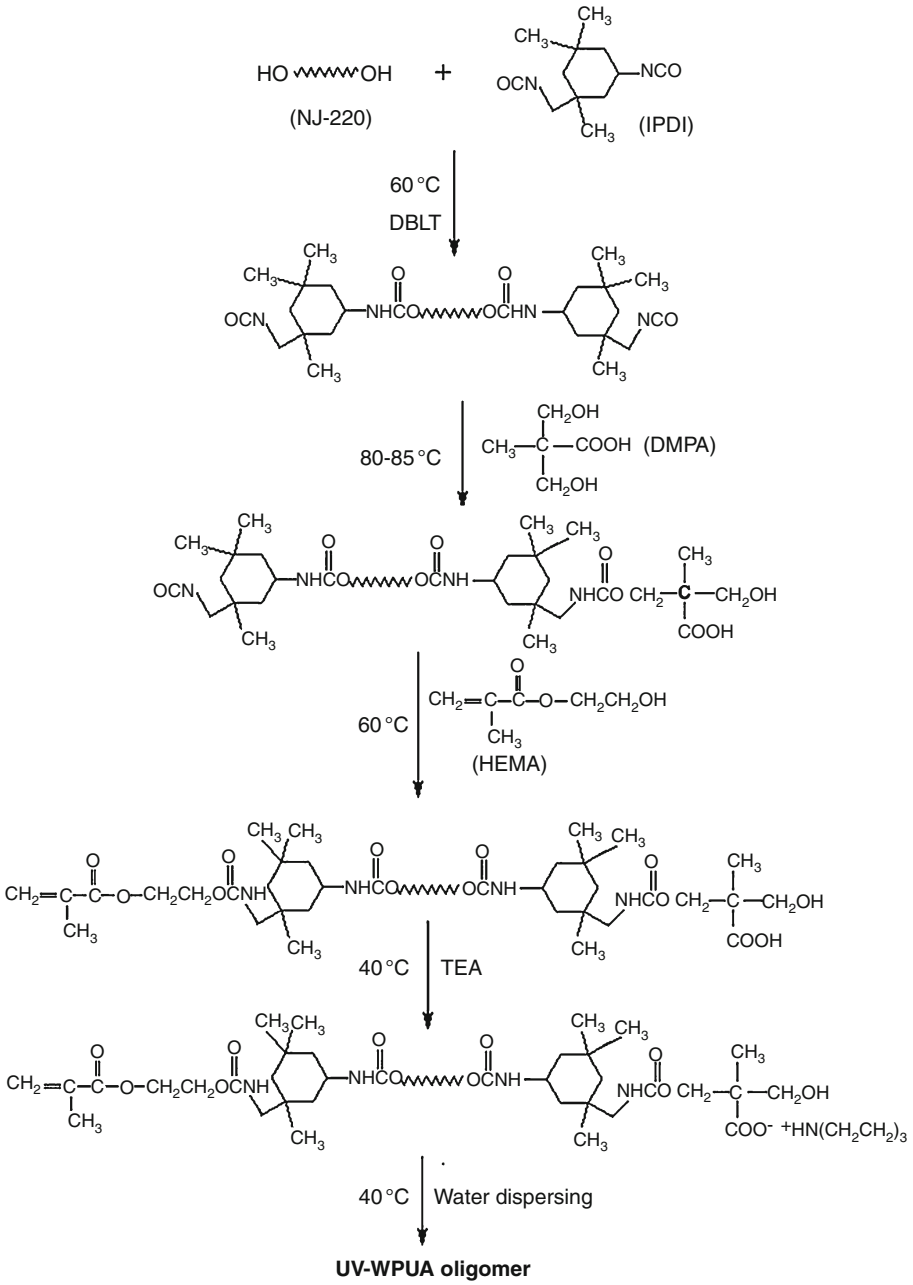

Fig. 1: Synthetic route of UV-WPUA oligomer

moiety, and the polymerization of the epoxy group simultaneously. The epoxy group of GLYMO can be reacted with the –OH groups of DMPA and HEMA; GLYMO has the ability to simultaneously form an organic network through the reaction of the organic functional groups with the organic binder and also an inorganic SiO_2 network through the hydrolysis and subsequent condensation reactions of alkoxy silane groups. Therefore, with various proportions of GLYMO and TEOS, a series of UV-WPUA/SiO_2 hybrid oligomers was obtained.

In this work, the hybrids with different TEOS contents of 0.1, 0.2, 0.3, 0.4, and 0.5 wt% were expressed as UV-Hyb-1, UV-Hyb-2, UV-Hyb-3, UV-Hyb-4, and UV-Hyb-5, respectively, as shown in Table 1. The synthetic route of the UV-WPUA/SiO_2 hybrid oligomer is shown in Fig. 2.

Preparation of UV-WPUA$_0$ and UV-WPUA/SiO$_2$ hybrid coating films

UV-WPUA$_0$ or UV-WPUA/SiO_2 hybrid coating films were prepared by casting the newly synthesized WPUA oligomer or UV-WPUA/SiO_2 hybrid oligomers with different TEOS contents (50 wt%), butyl acrylate (BA, 23.5 wt%), tripropyleneglycol diacrylate (TPGDA, 23.5 wt%), and Darocur 1173 (3 wt%) onto a poly(tetrafluoroethylene) drying at 65°C for 3 h. Because water was used as a diluent in this system, it needed the flash-off step, in which water is evaporated before UV curing. During aqueous dispersion to dry film, physical entanglement occurred, then tack-free film could be acquired because of the large molecular weight of the prepolymer.[11,12] Then, with the UV light that was produced by a lamp (main wave length: 365 nm, power of lamp: 1000 W, distance between thin film samples and center of UV lamp: 20 cm, and light intensity at the sample: 250 mW/cm^2), the Darocur 1173 was activated and the radicals could be produced. The formed radicals broke the acrylate double bond of the monomers and oligomers, which resulted in cross-linking; then the UV-WPUA$_0$ and the UV-WPUA/SiO_2 films were obtained. In this work, the UV-WPUA$_0$ and UV-WPUA/SiO_2 hybrid coating films were expressed as UV-WPUA$_0$, UV-Hyb$_{0.1}$, UV-Hyb$_{0.2}$, UV-Hyb$_{0.3}$, UV-Hyb$_{0.4}$, and UV-Hyb$_{0.5}$, respectively, as shown in Table 3.

The apparent viscosity of UV-WPUA and hybrid oligomers

The apparent viscosity of the UV-WPUA or UV-WPUA/SiO_2 aqueous oligomer was measured by a numerical viscometer (NDJ-9S, Shanghai Precision and Scientific Instrument Co. Ltd., Shanghai, China); when the shear rate was 2000 s^{-1}, the high shear rate guaranteed highly reliable measurements at a temperature of 25°C.

The particle size and polydispersity of UV-WPUA and hybrid oligomers

Particle size is the important parameter in deciding the end use industrial applications of aqueous polyurethane dispersions. The UV-WPUA or UV-WPUA/SiO_2 hybrid samples were added to 100-mL test tubes and diluted with deionized water. The particle diameter and polydispersity were measured by a laser

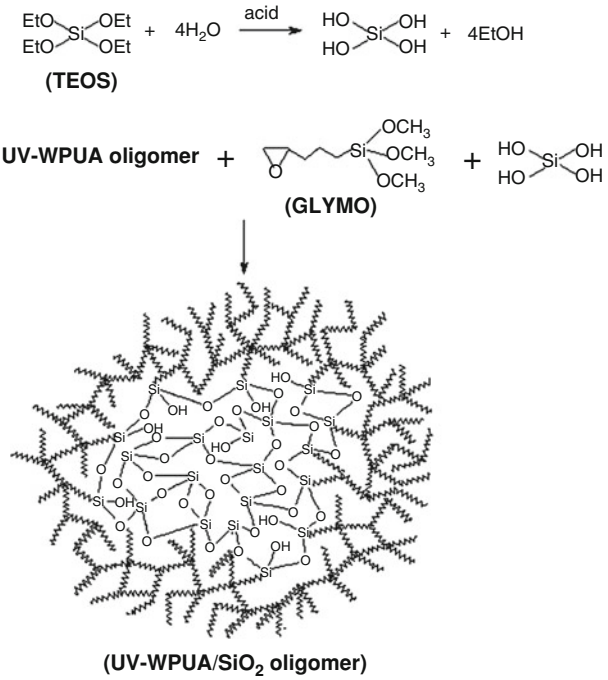

Fig. 2: Synthetic route of UV-WPUA/SiO_2 hybrid oligomer

Table 1: Reactant summaries of UV-WPUA and UV-hybrid oligomers

Sample	NCO/OH	DMPA (%)	NJ-220 (g)	IPDI (g)	GLYMO (g)	TEOS (wt%)
UV-WPUA	2/1	6.0	15.014	8.325	0	0
UV-Hyb-1	2/1	6.0	15.014	8.325	0.413	0.1
UV-Hyb-2	2/1	6.0	15.014	8.325	0.826	0.2
UV-Hyb-3	2/1	6.0	15.014	8.325	1.239	0.3
UV-Hyb-4	2/1	6.0	15.014	8.325	1.652	0.4
UV-Hyb-5	2/1	6.0	15.014	8.325	2.065	0.5

particle size analyzer (BIC-9010, Brookhaven Instrument Co., Holtsville, NY, USA).

Structure characterization of the UV-WPUA and hybrid oligomers

The FTIR spectrum of the oligomer was obtained between 4000 and 400 cm^{-1} with an FTIR spectrometer (AVATAR 360, Madison, Nicolet) using KBr pellets. A minimum of 32 scans was signal-averaged with a resolution of 2 cm^{-1} in the 4000–400 cm^{-1} range.

The surface drying time of UV-WPUA$_0$ and hybrid coating films

The UV-WPUA$_0$ or UV-WPUA/SiO_2 hybrid emulsion was put onto a poly(tetrafluoroethylene) drying at 65°C for 3 h. The water was evaporated before UV curing. Then dried film was cured by a UV lamp (main wave length: 365 nm, power of lamp: 1000 W, distance between thin film samples and center of UV lamp: 20 cm, and light intensity at the sample: 250 mW/cm^2). The UV-curable film was gently pressed with a finger. If there was no trace on the film, the time of the UV lamp irradiating was the surface drying time of the UV-WPUA$_0$ and UV-WPUA/SiO_2 films.

The gel content of UV-WPUA$_0$ and hybrid coating films

The UV-WPUA$_0$ or hybrid coating film was cut into 2 cm × 2 cm squares to determine its weight (W_0) and then put into the sorbite extractor with toluene as the solvent for 48 h; the rest weight (W) of the film was obtained after drying for 72 h at 30°C. Then the gel content was calculated according to the following formula:

$$G = \frac{W}{W_0} \times 100\% \quad (1)$$

The hardness of UV-WPUA$_0$ and hybrid coating films

The hardness of the film was measured with a sclerometer (KYLX-A, Jiangdu Kaiyuan Test Machine Co. Ltd., Jiangdu, China); measurements were done three times for each sample, and the average value was calculated.

The tensile strength and elongation at break of UV-WPUA$_0$ and hybrid films

Tensile strength testing and elongation at break testing for all of the specimens were carried out on a tensile tester (KY-8000A, Jiangdu Kaiyuan Test Machine Co., Ltd. Jiangdu, China) at room temperature at a speed of 50 mm/min. All measurements had an average of three runs. The dumbbell-type specimen was 30 mm long at two ends, 0.2 mm thick, and 4 mm wide at the neck.

The water absorption (or swelling degree) of UV-WPUA$_0$ and hybrid films

The water absorption (or swelling degree) was examined by preparation of dried films (30 mm × 30 mm; original weight designated as m_1) immersed in water, or 5 wt% NaOH, or ethanol, for 24 h at 25°C. After the residual water was wiped from the films using filter paper, the weight (m_2) was measured immediately. The water absorption or swelling degree (ω) was calculated as follows:

$$\omega = \frac{m_2 - m_1}{m_1} \times 100\% \quad (2)$$

Thermal properties

Differential scanning calorimetry (DSC) and thermogravimetric analysis (TGA) of the film were performed on a Netzsch instrument (STA 449C, Netzsch, Seligenstadt, Germany). The programmed heating range was from room temperature to 500°C at a heating rate of 10°C/min under a nitrogen atmosphere. The measurement was taken with 6–10 mg samples. DSC and TG curves were recorded.

SEM

To investigate the morphology of the film, the fracture surface was investigated with a 20-kV accelerating voltage with a field emission scanning electron microscope (S-4800, Hitachi Corp., Tokyo, Japan).

TEM

The morphology of the composite particles was observed by TEM (TECNAI-12, Philips Co., Eindhoven, The Netherlands) with an acceleration voltage of 120 kV. The composite particles were dispersed in deionized water in an ultrasonic bath for 10–30 min and then prepared by the deposition of the emulsion onto a copper net after it was stained by phosphorwolframic acid.

XRD

The XRD pattern was recorded by the reflection scan with nickel-filtered Cu Kα radiation (D8, Bruker-AXS, Karlsruhe, Germany). The X-ray generator was run at

50 kV and 70 mA. All of the XRD measurements were performed at 2θ values between 3 and 60.

Results and discussion

The physical properties of UV-WPUA and hybrid oligomers

The physical properties of UV-WPUA and UV-WPUA/SiO_2 oligomers are listed in Table 2. The viscosity of a UV-curable system is considered one of the most important parameters, affecting the processability and the photopolymerization rate of the cured film. So a suitable viscosity of the UV-curable system is very important to the properties of the final cured film. Table 2 shows the viscosity of the UV-WPUA and UV-WPUA/SiO_2 hybrid oligomers. It was found that the viscosity of the UV-WPUA/SiO_2 oligomers was smaller than that of the UV-WPUA oligomer, because of improvement of the compatibility of the hybrid with the coupling agent GLYMO and better distributive performance and lower scattering property for UV rays. The results indicated that the organic and inorganic components were miscible.[13] In addition, with the content of the TEOS increasing, the viscosity increased gradually, because of the DMPA and epoxysilane (GLYMO) acting as an internal emulsifier and a coupling agent, respectively, which made the UV-WPUA/SiO_2 hybrid oligomer very stable.

The hybrid oligomers had a maximum diameter of 113.2 nm (UV-Hyb-5), and the particle became bigger with the content of the TEOS increasing. This was mainly due to the inclusion of silica nanoparticles, which has been verified in waterborne silica nanocomposites using the phase-inversion-emulsification technique.[14] The epoxy on GLYMO reacts with the DMPA and HEMA stabilizing the UV-WPUA, and this leads to coagulation of some particles and an increase in overall particle size. In addition, the polyurethane chain containing NJ-220 soft segments could adsorb the silica and encapsulate the silica particles. With the increase in the particle size, the appearance of the emulsion changes from semitransparent to opaque.[15] The polydispersity of UV-WPUA and the hybrid oligomer dispersion showed little difference.

The gel content and the surface drying time of UV-WPUA$_0$ and hybrid coating films

The gel content and the surface drying time of UV-WPUA$_0$ and the UV-WPUA/SiO_2 hybrid coating films are shown in Fig. 3. In order to remove soluble fractions from the UV-cured WPUA and hybrid films, each sample was extracted with toluene. As seen in Fig. 3, when the TEOS amount was below 0.2 wt%, the gel content was increased only slightly from 84.06 to 85.11 wt%, and then ramped up quickly to 90.93 wt% between 0.2 and 0.3 wt%. After more than 0.3 wt% TEOS was used, the gel content was again increased, but slowly, in the range from 92.17 to 92.97 wt%. These results confirm the strong relation between the WPUA and silica components.

As a characterization factor of the surface curing degree of the coating, the surface drying time is used to evaluate the introduction of nanosilica on the surface UV curing of the membrane in the air.[16] As seen in Fig. 3, the surface drying time of the hybrid coating film was longer than that of the UV-WPUA$_0$, and with the content of the TEOS increasing, the surface drying time increased. This was due to the crosslinking density and the number of the nanosilica porous structure increasing, resulting in the content of the dissolved oxygen acting as an inhibitor to the UV curing of the

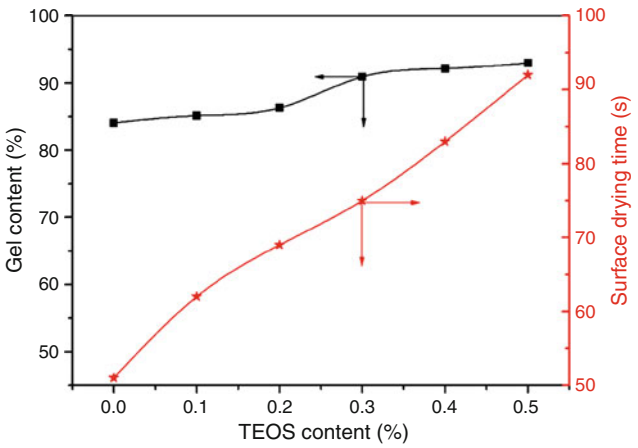

Fig. 3: Gel content and the surface drying time of UV-WPUA$_0$ and hybrids

Table 2: The physical properties of UV-WPUA and WPUA/SiO_2 oligomers

Sample	Apparent viscosity (mPa·s)	Particle size (nm)	Polydispersity	Appearance
UV-WPUA	0.236	37.6	0.318	★, #, ■
UV-Hyb-1	0.203	47.2	0.331	★, #, ■
UV-Hyb-2	0.205	81.8	0.328	★, #, ■
UV-Hyb-3	0.213	106.5	0.320	☆, #, ■
UV-Hyb-4	0.215	107.7	0.316	☆, ※, ■
UV-Hyb-5	0.230	113.2	0.286	☆, ※, ■

★: slightly white; ☆: milkiness; #: semitransparent; ※: opaque; ■: microblue

Table 3: The mechanical properties of UV-WPUA$_0$ and hybrid coating films

Sample	Oligomer	Hardness (shore A)	Tensile strength (MPa)	Elongation at break (%)
UV-WPUA$_0$	UV-WPUA	89	1.89	59.26
UV-Hyb$_{0.1}$	UV-Hyb-1	90	3.31	50.31
UV-Hyb$_{0.2}$	UV-Hyb-2	92	3.69	77.24
UV-Hyb$_{0.3}$	UV-Hyb-3	93	3.04	84.11
UV-Hyb$_{0.4}$	UV-Hyb-4	94	2.43	63.97
UV-Hyb$_{0.5}$	UV-Hyb-5	92	3.25	82.68

free radicals became more and more, so that the surface drying time increased.[17–19]

The mechanical properties of UV-WPUA$_0$ and hybrid coating films

The mechanical properties of the UV-WPUA$_0$ and UV-WPUA/SiO_2 hybrid coating films are shown in Table 3. The hardness value of the UV-WPUA/SiO_2 hybrid coating material was slightly higher than that of the UV-WPUA$_0$. This was due to the polycondensation that was generated by the hydroxyl from the SiO_2 surface and the hydrolysis of the coupling agent GLYMO, which improved the effect of the interface between the organic and inorganic phases and could increase the hardness. With the content of the SiO_2 increasing, the structure of the interpenetrating polymer network became much denser and the hardness of the materials increased. However, the hardness of the hybrid materials did not increase further when the SiO_2 content continued to increase (e.g., UV-Hyb$_{0.5}$). This was because only when the added amount of SiO_2 was small could it make the hardness of the membranes improve. Therefore, when the amount of SiO_2 increased to a certain extent, the nanoparticles showed a nonuniform dispersed phase, and the hybrids had a decreased toughness.

The tensile strength and elongation at break of the UV-WPUA/SiO_2 hybrids were higher than those of the UV-WPUA$_0$. The improvement of the mechanical properties could be explained by the results of the formation of the crosslinking.[20] When the content of the TEOS increased, the interpenetrating polymer network structure of the UV-WPUA/SiO_2 film was more compact. There was also some crosslinking of the PUA with the BA phase through the HEMA capping agent. On the whole, the tensile strength increased while the content of the TEOS increased from 0 to 0.2 wt%. However, the tensile strength decreased when the content of the TEOS was more than 0.2 wt%. The excessive nanosilica particles are detrimental to tensile strength improvement. The nanosilica can improve the mechanical properties of WPU films by increasing the crosslinking density of the polymer. Increasing the content of the TEOS leads to higher crosslinking density between crosslinking points. Excessive crosslink structure of the macromolecule leads to the increasing particle size of the PUA emulsion and the emulsion will be unstable due to the severe aggregation (see ''TEM'' section) of the sample. Unstable PUA emulsion is a great hindrance to the film-forming properties, which results in the decrease in tensile strength of the films.[21]

It was especially interesting that the elongation at break also increased initially with the TEOS content as with the tensile strength. This was mainly because the elongation at break of composites usually decreases with increasing of the reinforcement and the deformation mechanism of PUA.[22,23] In the case of PUA composed of hard and soft segment domains, the hard segment lamellae sensitive to applied stress can be tilted toward the stretching direction under low strain, and under high strain, they align parallel to the stretching direction. Thus PUA can maintain its stress capacity under relatively high strain without any breakdown of amorphous soft chains. The UV-WPUA–silica hybrids in our study may endure higher tensile strength due to the incorporation of silica, though an excess of silica negatively affected elongation of the sample. That is, as the TEOS content increased initially, the formed silica gradually reinforced the composite without hindering elastic deformation of the soft segments, resulting in higher breaking strength and elongation at break. However, the incorporation of an excess of silica hindered the deformation of soft segments in UV-WPUA and thus led to lower elongations at break.[23] In summary, the mechanical properties of the hybrid films were improved by the modification of the coupling agent and a certain amount of TEOS.

The water absorption (or swelling degree) of UV-WPUA$_0$ and hybrid coating films

The water absorption or swelling degree of the UV-WPUA$_0$ and UV-WPUA/SiO_2 hybrid coating films was measured, and the results are shown in Table 4. Water absorption values of the hybrids revealed that those containing silica precursors caused slightly increased water uptakes compared to the control formulation. This result suggests that the residual polar

Table 4: The water absorption (or swelling degree) of UV-WPUA$_0$ and hybrid coating films

Sample	Water absorption (%)	Swelling degree (%) (5% NaOH)	Swelling degree (%) (ethanol)
UV-WPUA$_0$	1.29	4.15	12.48
UV-Hyb$_{0.1}$	1.85	2.08	8.39
UV-Hyb$_{0.2}$	1.93	7.52	3.82
UV-Hyb$_{0.3}$	1.62	6.15	5.88
UV-Hyb$_{0.4}$	1.55	9.15	4.32
UV-Hyb$_{0.5}$	1.17	2.32	9.02

groups derived from sol–gel silane solution in the hybrid systems presented an affinity towards water. With the content of the TEOS increasing, the water absorption first increased. This increase for these materials was attributable to an increase in the hydrophilic nature of the polymer backbone due to the hydroxyl groups. It could be clearly seen that the TEOS-derived materials showed the highest gain in hydroxyl uptake. This absorption occurred even at very low volume fractions of TEOS. The increase in water absorption for the TEOS-based PUA was attributed to the high concentration of siloxane groups. Also, an interesting fact regarding TEOS was their inherent porosity. This porosity should cause increments in the water uptake results. TEOS-derived materials demonstrated how porosity and hydrophilic character could increase the water absorbency in a hybrid material. In addition, the specific surface area of the nanosilica itself was very large, so the water absorption first increased. However, with the content of the TEOS increasing, the structure of the interpenetrating polymer network became much denser, which would prevent the water from absorbing. Since the polymeric material had a strong insulating property in the crosslinking process because of the addition of siloxane to the polymer structure, usually water absorption decreased. The main reason for water absorption was usually because of the penetration of the suitable sorption sites by water and this caused a decrease in selectivity. In this work, when the content of the TEOS was 0.5 wt%, the water absorption of the hybrid material was minimal, and at that moment the hybrid material had the best water resistance.[24]

Compared with the UV-WPUA$_0$, the UV-Hyb$_{0.1}$ and the UV-Hyb$_{0.5}$ had better alkalinity resistances, while the ethanol resistances of the UV-Hyb materials were excellent.

Structure characterization, thermal properties, and morphology characterization of UV-WPUA$_0$ and hybrids

The structure of the UV-WPUA and WPUA/SiO_2 oligomers were categorized by FTIR, as shown in Fig. 4. The spectral analysis was used mainly to check the completion of the polymerization reaction, in terms of the disappearance of the –NCO band at 2270 cm^{-1}, and the appearance of the N–H band at 3310–3500 cm^{-1}. The result indicated that the NCO had reacted with OH into NHCOO and the NCO groups had been completely reacted. There was a strong absorption peak at about 1680 cm^{-1}, which corresponded to the carbamate carbonyl of –C=O groups. The absorption peaks typically at 1460 cm^{-1} (=CH_2), indicating that the C=C bond of HEMA had been grafted into the polyurethane chains. Clearly, there were wide and strong absorption peaks from 1050 to 1150 cm^{-1} in the samples of the hybrid materials, showing the existence of an Si–O–Si backbone, which was due to the polycondensation between the siloxane side of the coupling agent GLYMO and the hydrolysis of the TEOS, which formed the Si–O–Si network and generated an interpenetrating polymer network between the organic and inorganic phases. In addition, there was an absorption peak at about 930 cm^{-1}, which corresponded to the Si–O–C bond in the samples of the hybrid materials, indicating that it was not a simple mixture of silicon dioxide and WPUA but the bonding of some kind of chemical bond. Therefore, it formed a strong bond-linked complex hybrid interaction system between the organic polymer and the inorganic phase, which weakened the key single phase body and provided the basis for the excellent performance of the hybrid materials.

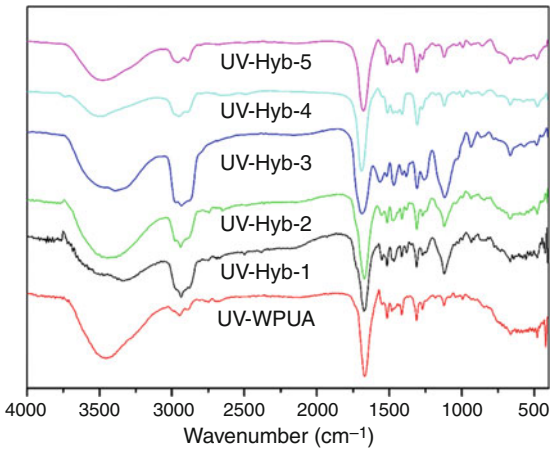

Fig. 4: FTIR spectra of UV-WPUA and hybrid oligomers

The DSC and TGA curves for the UV-WPUA$_0$ and WPUA/SiO_2 hybrids are shown in Figs. 5 and 6. In Fig. 5, it can be seen from the DSC curves that a glass transition temperature (T_g) peak appeared in the range of 40–80°C and was related to the hard segment T_g. The result indicated that the hybrids had a strong and uniform interaction between WPUA and SiO_2 nanoparticles, which was due to the bridge effect by the GLYMO. On the other hand, the result indicated that the organic polymers were almost completely compatible, because of the copolymerization between the

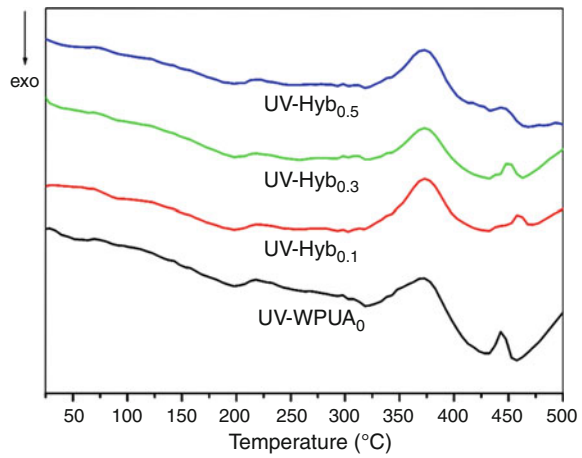

Fig. 5: DSC curves of UV-WPUA$_0$ and hybrids

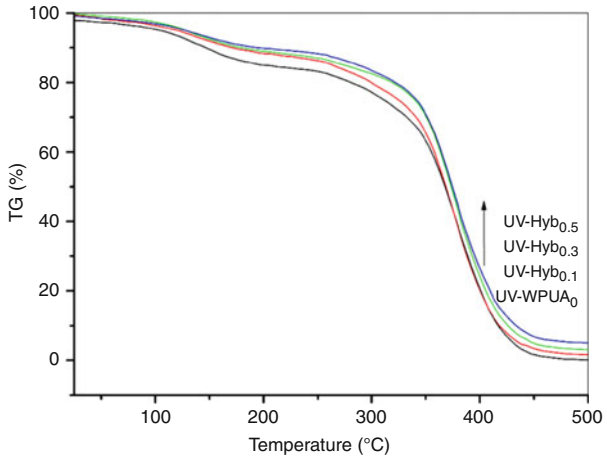

Fig. 6: TGA curves of UV-WPUA$_0$ and hybrids

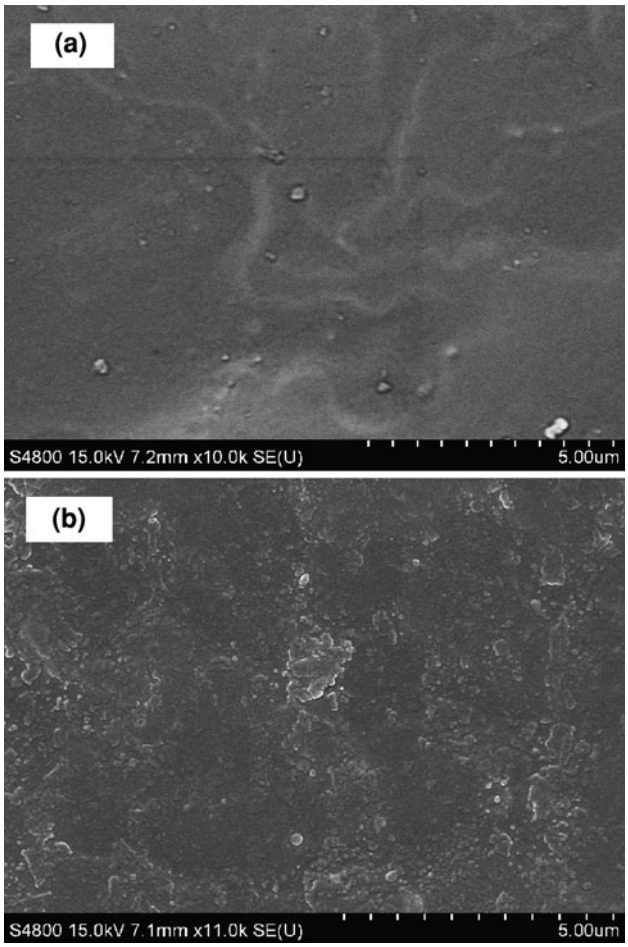

Fig. 7: SEM photographs of UV-WPUA$_0$ (a) and UV-Hyb$_{0.3}$ (b)

organic polymer WPUA and the inorganic components, greatly improving the compatibility. The hybrid materials had a higher glass transition temperature (T_g) of the hard segments than the pure UV-WPUA$_0$. The T_g of the hybrid accessed by DSC was also slightly increased as the TEOS content was increased. This was clearly caused by the strong interaction between the SiO_2 and the PUA, which limited the segmental movement of the PUA.

As seen in Fig. 6, the materials had a slight weight loss at relatively low temperature (less than 150°C). This was mainly because the water on the surface of the materials evaporated. The weight loss at around 150–300°C was probably due to the evaporation of strongly absorbed water and condensation by-products of the organic alkoxy silane compound. This step, corresponding to the maximum weight loss in the range of 300–500°C, was attributed to the decomposition of the polymer chain. As seen from the TGA curves, the higher the TEOS content in the hybrid system, the more char residue was observed. From the above analysis, we see that the UV-WPUA/SiO_2 materials had a good thermal property.

SEM is used to visually evaluate the dispersion of silica nanoparticles in a waterborne polyurethane acrylate matrix. The micrograph sections of UV-WPUA$_0$ (a) and UV-Hyb$_{0.3}$ (b) samples are shown in Fig. 7. A smooth WPUA film was observed in Fig. 7a with almost no cracks. In the case of the 0.3 wt% TEOS content, there were some cracks caused by the SiO_2 particles which were seen in the form of the majority of the white spots emerging at the bottom of the cracks in the UV-Hyb$_{0.3}$ material. The cracks showed that the fracture region extended along the SiO_2 particles, and the SiO_2 particles dispersed in the body of UV-Hyb material. In addition, the particles were uniformly dispersed in the UV-Hyb system and the inorganic SiO_2 particles were embedded in the organic–inorganic network structure, which explains why the inorganic particles were besieged by the organic phase acting as the continuous phase (see Fig. 7b).

TEM micrographs of the UV-WPUA$_0$ and hybrids are shown in Fig. 8. A large number of nanosilica particles dispersed uniformly in the WPUA matrix,

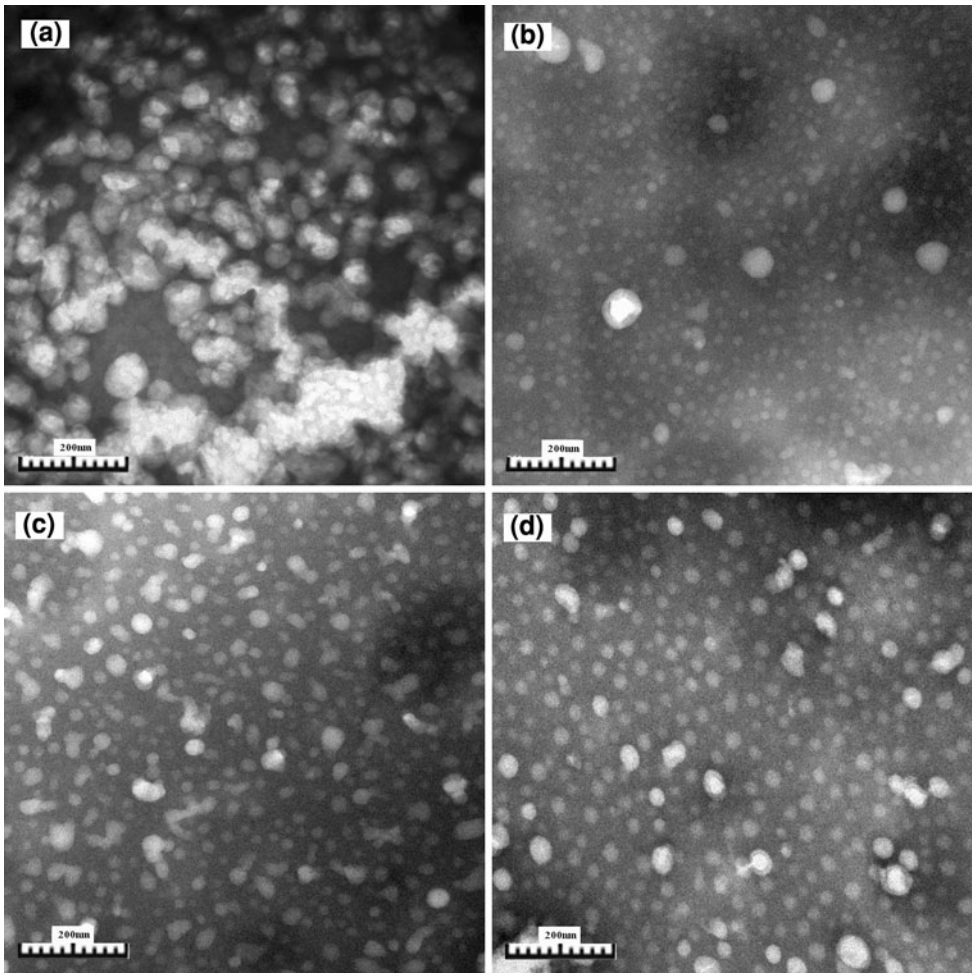

Fig. 8: TEM photographs of UV-WPUA$_0$ (a), UV-Hyb$_{0.1}$ (b), UV-Hyb$_{0.3}$ (c), and UV-Hyb$_{0.5}$ (d)

which was mainly due to the regular molecular network structure of the WPUA effectively limiting the nanosilica. On the other hand, covalent bonding (Si–O–Si) between the organic and inorganic components, which was homogeneously and uniformly dispersed, enhanced the miscibility. The formation of SiO_2 particles in the prepared WPUA and coupling agent GLYMO matrix indicated that the $-Si(OCH_3)_3$ groups may have functioned as internal bridging groups between the organic and inorganic segments for sol–gel reactions of the TEOS molecules. The condensation reaction steps of TEOS in the WPUA solution were in the following sequence: nucleation, nucleus propagation forming colloids, and particle growth through colloid collision. However, the WPUA chain in solution inhibited the particle growth, and the size slightly increased as the SiO_2 content increased. The increase in the SiO_2 particle size clearly resulted from the increase in the aggregation tendency, as the TEOS content and the SiO_2 particle number increased. These micrographs show the fine interconnected or continuous phase morphologies, and these materials would be adequate for practical applications.

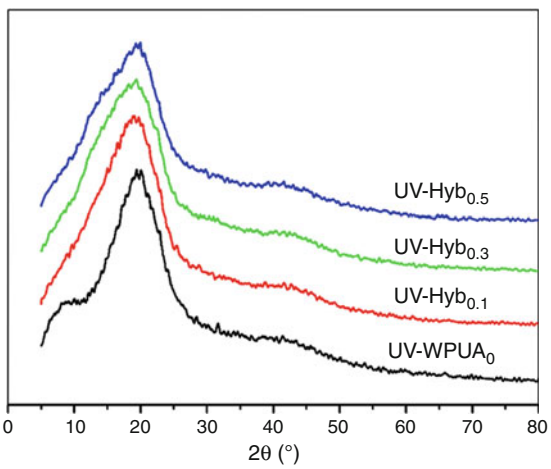

Fig. 9: X-ray diffractograms of UV-WPUA$_0$ and hybrids

X-ray diffraction analyses of the UV-WPUA$_0$ and UV-WPUA/SiO_2 hybrid films are shown in Fig. 9. For the pure UV-WPUA$_0$ film, a broad diffraction halo was observed near $2\theta = 20°$, and this diffraction halo was

associated with the amorphous phase of the PUA.[25] In addition, a diffused diffraction peak appeared near 20° for all of the hybrid nanocomposites, and this peak was attributed to the short-range-order arrangement of chain segments of amorphous PUA and the formation of a uniform three-dimensional network structure, which was interspersed with the WPUA segment. The nanosilica did not display any crystalline peaks, which was consistent with the silica nanoparticles being noncrystalline at that size scale. It was observed that the peak of the hybrid films was slightly broader than that of the pure UV-WPUA$_0$ film. This influence further confirms that there exist strong interaction between the PUA and the silica nanoparticles for the nanostructured films.[26]

Conclusion

A series of UV-curable waterborne polyurethane acrylate/silica nanocomposites were successfully prepared by the in situ method and the sol–gel process. The average particle size and the viscosity of the UV-WPUA/SiO_2 dispersions increased with the increasing TEOS content. The hardness, tensile strength, and elongation at break of the UV-WPUA/SiO_2 hybrid films were better than those of pure UV-WPUA$_0$ film. When the content of the TEOS was 0.5 wt%, the UV curing hybrid had the best water resistance. The hybrid materials had a higher T_g of the hard segment than the pure UV-WPUA$_0$. The T_g of the hybrid films increased with an increasing TEOS content. The UV-WPUA/SiO_2 hybrids showed a homogeneous morphology, which supports the compatibility improvements shown by the SEM and TEM measurements.

Acknowledgments This project was supported by the Agricultural Independent Innovation of Jiangsu Province (CX(11)2032), Jiangsu Planned Projects for Postdoctoral Research Funds (1002033C) and Jiangsu Province Key Laboratory of Fine Petro-chemical Technology (213164).

References

1. Madbouly, SA, Otaigbe, JU, ''Recent Advances in Synthesis, Characterization and Rheological Properties of Polyurethanes and POSS/Polyurethane Nanocomposites Dispersions and Films.'' *Prog. Polym. Sci.*, **34** 1283–1332 (2009)
2. Berg, KJ, Ven, LGJ, Haak, HJW, ''Development of Waterborne UV-A Curable Clear Coat for Car Refinishes.'' *Prog. Org. Coat.*, **61** 110–118 (2008)
3. Xu, HP, Qiu, FX, Wang, YY, Wu, WL, Yang, DY, Guo, Q, ''UV-Curable Waterborne Polyurethane-Acrylate: Preparation, Characterization and Properties.'' *Prog. Org. Coat.*, **73** 47–53 (2012)
4. Yeh, JM, Yao, CT, Hsieh, CF, Yang, HC, Wu, CP, ''Preparation and Properties of Amino-Terminated Anionic Waterborne-Polyurethane–Silica Hybrid Materials Through a Sol–Gel Process in the Absence of an External Catalyst.'' *Eur. Polym. J.*, **44** 2777–2783 (2008)
5. Vollath, D, Szabo, DV, Schlabach, S, ''Oxide/Polymer Nanocomposites as New Luminescent Materials.'' *J. Nanopart. Res.*, **6** 181–191 (2004)
6. Cho, JD, Ju, HT, Hong, JW, ''Photocuring Kinetics of UV-Initiated Free-Radical Polymerizations With and Without Silica Nanoparticles.'' *J. Polym. Sci. Part A Polym. Chem.*, **43** 658–670 (2005)
7. Karataş, S, Kızılkaya, C, Kayaman-Apohan, N, Güngör, A, ''Preparation and Characterization of Sol–Gel Derived UV-Curable Organo-Silica–Titania Hybrid Coatings.'' *Prog. Org. Coat.*, **60** 140–147 (2007)
8. Huang, HC, Hsieh, TE, ''Preparation and Characterizations of Highly Transparent UV-Curable ZnO-Acrylic Nanocomposites.'' *Ceram. Int.*, **36** 1245–1251 (2010)
9. Bayramoğlu, G, Kahraman, MV, Kayaman-Apohan, N, Güngör, A, ''Synthesis and Characterization of UV-Curable Dual Hybrid Oligomers Based on Epoxy Acrylate Containing Pendant Alkoxysilane Groups.'' *Prog. Org. Coat.*, **57** 50–55 (2006)
10. Suryani, Liu, YL, ''In Situ Sulfonation and Formation of Polybenimidazole Nanocomposite Membranes Using Sulfonated Silica Nanoparticles for Fuel Cell Applications.'' *J. Membr. Sci.*, **332** 121–128 (2009)
11. Ahn, YU, Lee, SK, Lee, SK, Jeong, HM, Kim, BK, ''High Performance UV Curable Polyurethane Dispersions by Incorporating Multifunctional Extender.'' *Prog. Org. Coat.*, **60** 17–23 (2007)
12. Lee, MH, Choi, HY, Jeong, KY, Lee, JW, Hwang, TW, Kim, BK, ''High Performance UV Cured Polyurethane Dispersion.'' *Polym. Degrad. Stab.*, **92** 1677–1681 (2007)
13. Ma, GZ, Liu, W, Yan, T, Wei, LQ, Xu, BS, ''Preparation of Polymeric Nanosilica Hybrid Materials and Their Properties.'' *Acta Polym. Sin.*, **2** 203–209 (2011)
14. Nunes, RCR, Pereira, RA, Fonseca, JLC, Pereira, MR, ''X-Ray Studies on Compositions of Polyurethane and Silica.'' *Polym. Test.*, **20** 707–712 (2001)
15. Masakazu, H, Zhou, J, Katsutoshi, N, ''The Structure and Properties of Acrylic–Polyurethane Hybrid Emulsions.'' *Prog. Org. Coat.*, **38** 27–34 (2000)
16. Lombardi, V, Bongiovanni, R, Malucelli, G, Priola, A, Garavaglia, S, Turri, S, ''New Acrylic–Allylic Resins Containing Perfluoropolyether Chains for UV-Cured Coatings.'' *Pigm. Resin Technol.*, **28** 212–216 (1999)
17. Rahman, MM, Khan, MA, Mustafa, AI, ''Role of Sand on Curing of Partex Surface by UV Radiation.'' *J. Appl. Polym. Sci.*, **86** 2385–2392 (2002)
18. Mani, S, Cassagnau, P, Bousmina, M, Chaumont, P, ''Cross-Linking Control of PDMS Rubber at High Temperatures Using TEMPO Nitroxide.'' *Macromolecules*, **42** 8460–8467 (2009)
19. Avens, HJ, Bowman, CN, ''Mechanism of Cyclic Dye Regeneration During Eosin-Sensitized Photoinitiation in the Presence of Polymerization Inhibitors.'' *J. Polym. Sci. Part A Polym. Chem.*, **47** 6083–6094 (2009)
20. Wang, LW, Ye, T, Ding, HY, Li, JD, ''Microstructure and Properties of Organosoluble Polyimide/Silica Hybrid Films.'' *Eur. Polym. J.*, **42** 2921–2930 (2006)
21. Wang, L, Shen, YD, Lai, XJ, Li, ZJ, ''Effect of Nanosilica Content on Properties of Polyurethane/Silica Hybrid Emulsion and its Films.'' *J. Appl. Polym. Sci.*, **119** 3521–3530 (2011)
22. Cho, JW, Lee, SH, ''Influence of Silica on Shape Memory Effect and Mechanical Properties of Polyurethane–Silica Hybrids.'' *Eur. Polym. J.*, **40** 1343–1348 (2004)

23. Valentova, H, Sedlakova, Z, Nedbal, J, Ilavsky, M, ''Formation, Structure, Thermal and Dynamic Mechanical Behaviour of Ordered Polyurethane Networks Based on Mesogenic Diol.'' *Eur. Polym. J.*, **37** 1511–1517 (2001)
24. Boroglu, MS, Gurkaynak, MA, ''The Preparation of Novel Silica Modified Polyimide Membranes: Synthesis, Characterization, and Gas Separation Properties.'' *Polym. Adv. Technol.*, **22** 545–553 (2011)
25. Bonilla, G, Martınez, M, Mendoza, AM, Widmaier, JM, ''Ternary Interpenetrating Networks of Polyurethane–Poly(methyl methacrylate)-silica: Preparation by the Sol–Gel Process and Characterization of Films.'' *Eur. Polym. J.*, **42** 2977–2986 (2006)
26. Zhang, S, Jin, R, Jiang, Q, Yang, C, Chen, M, Liu, X, ''Facile Synthesis of Waterborne UV-Curable Polyurethane/Silica Nanocomposites and Morphology, Physical Properties of Its Nanostructured Films.'' *Prog. Org. Coat.*, **760** 1–8 (2011)